Advancing landscape characterisation: a comparative study of machine learning and manual classification methods

Ecological Informatics 90 (2025) 103349

Contents lists available at ScienceDirect

Ecological Informatics

journal homepage: www.elsevier.com/locate/ecolinf

Advancing landscape characterisation: A comparative study of machine learning and manual classification methods

Tingting Huang [a,b], Geoffrey Griffiths [b,e,*], Bo Huang [c,d,*], Jianning Zhu [a,*], Steven Warnock [e], Martin Lukac [b,f,*]

[a] School of Landscape Architecture, Beijing Forestry University, Beijing 100083, China
[b] School of Agriculture, Policy and Development, University of Reading, Reading RG6 6UR, UK
[c] College of Optoelectronic Engineering, Chongqing University, Chongqing 400044, China
[d] Key Laboratory of Optoelectronic Technology and Systems of the Education Ministry of China, Chongqing University, Chongqing 400044, China
[e] Landscape Matters, Evesham, OX7 3DA, UK
[f] Faculty of Forestry and Wood Sciences, Czech University of Life Sciences Prague, Prague, 165 00, Czechia

ARTICLE INFO

Dataset link: https://github.com/TingtingHwang/BBNP_LCA

Keywords:
Landscape character classification
Automated classification
Machine learning
Swin transformer
Landscape mapping

ABSTRACT

This study evaluates and compares three automated classification methods for Landscape Character Assessment (LCA) to assess their suitability for consistent, objective, and scalable mapping. We applied One-pass Multi-view Clustering (OPMC), Self-Organising Feature Map (SOFM) clustering, and Swin Transformer Segmentation Clustering (STSC) to classify Landscape Character Types in Bannau Brycheiniog National Park, Wales, UK. Their outputs were compared against an Expert-based Manual Classification (EBMC) using pixel-by-pixel accuracy assessment. To interpret model outputs, we used SHapley Additive exPlanations (SHAP) analysis to quantify the influence of key landscape character elements on classification outcomes. STSC showed the highest agreement with EBMC, followed by SOFM and OPMC. Across all models, geology, historic landscape, and soil type were the most influential variables, while habitat and landform contributed less. The automated methods demonstrated strong spatial coherence and boundary delineation comparable to expert-based mapping. Our findings demonstrate the potential of automated approaches to improve the consistency, efficiency, and objectivity of LCA and support their integration into scalable landscape characterisation frameworks for planning and management applications. Our source code and datasets are available on GitHub.

1. Introduction

Effective resource planning and environmental management increasingly require action at the landscape scale (Mücher et al., 2010; Warnock and Griffiths, 2015), particularly in the face of biodiversity loss, climate change, and rising demands for food and land (Buller et al., 2012). Landscapes are commonly defined as “distinct, recognisable, and consistent patterns of elements that make one landscape different from another”. They present a combination of tangible physical reality and how they are perceived and valued by people (Déjeant-Pons, 2006). Landscape Character Assessment (LCA) provides a structured approach for classifying, describing, and assessing landscapes based on their physical and cultural attributes and their development over time (Griffiths, 2018). It integrates biophysical and cultural elements to identify Landscape Character Types (LCTs), typically through expert interpretation and synthesis of mapped layers (Warnock and Griffiths, 2015; Van Eetvelde and Antrop, 2009). While manual LCA methods are effective at local scales, they can be time-consuming, subjective, and difficult to scale across larger or more varied regions (Simensen et al., 2018).

A successful LCA depends on a thorough understanding of the unique features, patterns, and dynamics of the landscape in question (Mücher et al., 2003). Landscape types often serve as the spatial framework for future management and planning efforts (Brown and Brabyn, 2012). The primary task enabling landscape mapping is to define character types that exhibit a reasonable degree of internal consistency in terms of their biophysical, cultural, and aesthetic characteristics (Capotorti et al., 2012). Due to the inherently multidisciplinary nature of landscape studies, encompassing geography, geomorphology, ecology, history, archaeology, and landscape architecture, different classification methods tend to prioritise different elements (Fairclough et al., 2018). This often leads to variability in the mapped outputs. For

* Corresponding authors.
E-mail addresses: huangtt17@bjfu.edu.cn (T. Huang), geoff.griffiths@reading.ac.uk (G. Griffiths), huangbo0326@cqu.edu.cn (B. Huang), blzjn0413@bjfu.edu.cn (J. Zhu), swarnock.livland@btinternet.com (S. Warnock), m.lukac@reading.ac.uk (M. Lukac).

https://doi.org/10.1016/j.ecoinf.2025.103349
Received 11 December 2024; Received in revised form 22 July 2025; Accepted 23 July 2025

landscape typologies to gain broader acceptance, they must be developed through repeatable procedures with clearly defined classification rules (Collier et al., 2012).

Advances in multivariate statistics and GIS overlay techniques have facilitated automated LCTs classification (Brabyn, 2009; Uzun et al., 2011; Warnock and Griffiths, 2015). However, challenges remain in achieving reproducibility and transferability, particularly when data availability varies or when applied to ecologically and culturally different landscapes (Sayre et al., 2014). Until recently, the LCA methodology largely remained an expert-led technique, relying on the visual interpretation of patterns in key attributes (Fairclough and Herring, 2016). Although LCA is theoretically transferable (Griffiths, 2018), its practical implementation depends heavily on the selection, quality, and consistency of input data. Transferability also remains constrained by differences in cultural and environmental contexts (Trop, 2017).

Automated classification techniques, including those based on machine learning and deep learning, offer considerable potential to address the limitations of traditional LCA. By enabling consistent and automated processing of complex spatial data, these approaches can reduce subjectivity and improve the reproducibility of classification outputs, potentially making them more objective than expert-led methods (Carvalho et al., 2019). Such techniques have already been widely applied in a range of disciplines, including soil science (Wang et al., 2020; Zhao et al., 2023), agriculture (Li et al., 2022), land management (Cui et al., 2023), ecology (Amani et al., 2023; Zhao et al., 2024), and landscape studies. Within this field, unsupervised classification methods are especially prominent. These methods group samples based on inherent similarities in the data, allowing for the identification of novel patterns without the need for prior labels or training data (Huang et al., 2023). In contrast, supervised classification relies on labelled training samples to learn known patterns and then classify new, unlabelled data accordingly (Antrop and Van Eetvelde, 2000).

The Expert-based Manual Classification (EBMC) used as a reference in this study was produced through the visual interpretation of multiple map layers, as described in Warnock and Griffiths (2015). This method involves the successive overlay of broad-scale physical elements, such as geology, soils, and topography, followed by further subdivision using cultural elements like settlement patterns, land use, woodland cover, and farm types, to delineate final landscape character types. While traditional LCA emphasises expert interpretation and perceptual dimensions, automated methods can identify the underlying biophysical template that provides the foundation for landscape character (Fagerholm et al., 2013). These approaches are complementary: data-driven methods establish objective baseline frameworks, while expert-based methods add perceptual interpretation.

In this study, we explore the potential of automated methods for landscape character classification, using Bannau Brycheiniog National Park (BBNP) in Wales, UK, as a case study. The park's varied and distinctive landscapes provide an ideal setting for testing scalable, data-driven approaches. We applied three machine learning models: One-pass Multi-view Clustering (OPMC), Self-Organising Feature Map (SOFM) clustering, and a semi-supervised deep learning model, Swin Transformer Segmentation Clustering (STSC), to identify LCTs. These models operate without predefined labels, relying instead on the intrinsic patterns in spatial and environmental data.

The objective of this study is to evaluate the effectiveness and limitations of these automated classification methods by comparing their outputs against the expert-based reference map. We assess the models' accuracy, spatial coherence, and ability to capture key landscape elements, with the aim of determining their suitability as scalable tools for landscape monitoring, conservation planning, and decision-making in protected areas such as BBNP.

2. Study area and data sources

2.1. Study area

This study was conducted using Bannau Brycheiniog National Park (BBNP) in south-central Wales as the study area. Covering 1347 km^2 (520 square miles), BBNP features a varied landscape of mountains, rivers, and forests (Fig. 1). Much of the park is upland terrain, rising to 886 m. The Usk River flows through its meadows and woodlands, creating a mosaic of habitats that support rich biodiversity. Beyond its ecological value, the park also holds cultural significance, containing numerous historical sites.

2.2. Data description

LCA relies on accurately identifying and mapping the heterogeneity of both natural and human-made characters, typically referred to as Landscape Character Elements (LCEs) (Turner and Gardner, 2015). Seven LCEs were used in this study: altitude, geology, soil type, landform, vegetation, habitat, and historic landscape (Table 1). Together, these datasets encompass 60 variables, as listed in Appendix A. Altitude data at 12.5 m resolution were obtained from NASA EARTHDATA (ALO, 2010). Geological information was sourced from the British Geological Survey at a 1:50,000 scale (BGS Digital Data Licence No. 2023/098; BGS, 2023). Soil type data came from the National Soil Map of England and Wales at a 1:250,000 scale, provided by the UK Soil Observatory and Cranfield University. Landform and historic landscape datasets were obtained from Natural Resources Wales. Vegetation and habitat data were sourced from the Living Wales project, offering a 10 m resolution (Owers et al., 2021). All datasets were projected to a common coordinate system and resampled to a uniform 30 m resolution using the Nearest Neighbour method.

With the increasing capability of GIS and the availability of 'big data', it is now possible to critically evaluate and prioritise the variables that contribute most to landscape variation. To assess multicollinearity among LCEs, we used two commonly applied metrics: Variance Inflation Factor (VIF) and Tolerance (TOL) (James et al., 2013). VIF quantifies how much the variance of a regression coefficient is inflated due to correlation with other variables. A VIF of 1 indicates no correlation, while values greater than 1 suggest increasing level of multicollinearity. A VIF above 10 is typically considered indicative of serious multicollinearity (Torres et al., 2020). TOL, defined as the reciprocal of VIF, provides a complementary measure. Low TOL values, especially in combination with high VIF values, signal potential multicollinearity problems. A widely used threshold for concern is $VIF > 10$ and $TOL < 0.1$ (Myers, 1990). The VIF and TOL were computed as follows,

$$VIF_j = \frac{1}{TOL} = \frac{1}{(1 - R_j^2)} \tag{1}$$

where R_j^2 represents the unadjusted coefficient of determination for regressing the jth independent variable on the remaining ones.

Table 1 confirms the absence of multicollinearity among the variables describing LCEs in this study, apart from historic landscape. All spatial data processing was conducted using ESRI ArcGIS Desktop 10.8.2, while multicollinearity analysis was carried out in MATLAB.

3. Methods

Following the collinearity analysis, the study progressed through two main analytical steps (Fig. 2):

(i) Automatic classification and validation: LCTs were identified using two unsupervised clustering models, One-pass Multi-view Clustering (OPMC) and Self-Organising Feature Map (SOFM), and one semi-supervised deep learning model, Swin Transformer Segmentation Clustering (STSC). The performance of these automated methods was

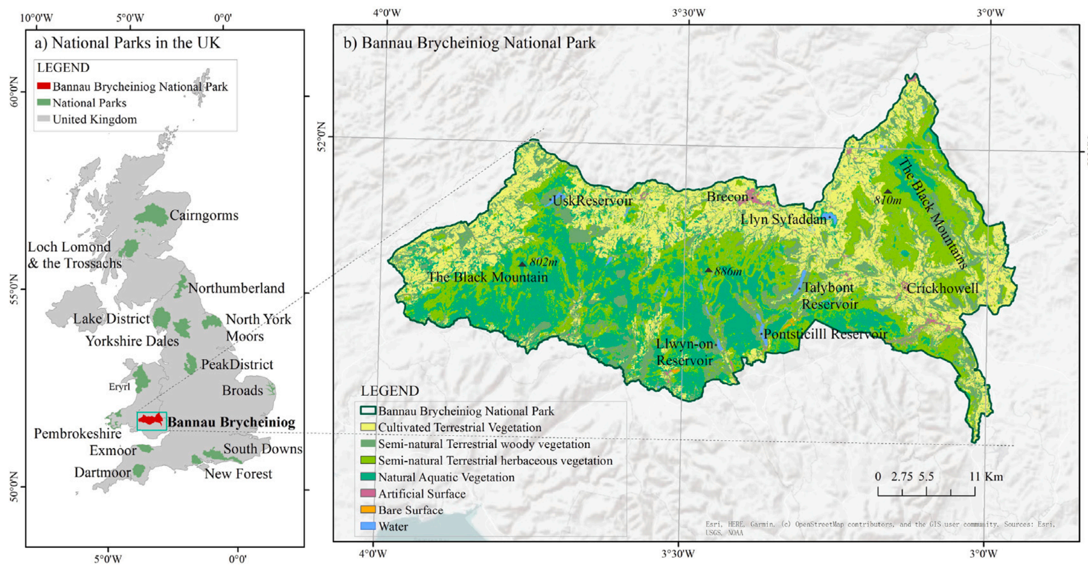

Fig. 1. Location of the study area: (a) National Parks in the UK and the location of the Bannau Brycheiniog National Park; (b) Habitat type of the Bannau Brycheiniog National Park.

Table 1
Landscape variables and multicollinearity analysis.

Variable name	Resolution	Time	Elements source	VIF	TOL
Altitude	Raster, 12.5 m	2023	NASA EARTHDATA (https://search.asf.alaska.edu/#/)	4.42	0.23
Geology	Vector, 1:50,000	2016	BGS Geology (https://www.bgs.ac.uk/datasets/bgs-geology-50k-digmapgb/)	9.06	0.11
Soil type	Vector, 1:250,000	2005	UK Soil Observatory, Cranfield (https://data.catchmentbasedapproach.org/datasets/theriverstrust)	7.24	0.14
Landform	Vector, 1:250,000	2017	Land map (https://datamap.gov.wales/)	8.34	0.12
Vegetation	Raster, 10 m	2021	Living Wales (https://earthtrack.aber.ac.uk/livingwales/maps.html)	5.99	0.17
Habitat	Raster, 10 m	2022	Living Wales (https://earthtrack.aber.ac.uk/livingwales/maps.html)	4.42	0.23
Historic landscape	Vector, 1:250,000	2017	Land map (https://datamap.gov.wales/layers/inspire-nrw)	10.37	0.10

then systematically compared against expert-based manual classification (EBMC). Cluster Validity Indices (CVI), specifically the Silhouette Coefficient (SC) and Davies–Bouldin (DB) index, were applied to determine the optimal number of clusters (k) for each method and assess clustering quality.

(ii) Results analysis: (a) SHapley Additive exPlanations (SHAP) were used to evaluate the contribution of each LCE to model outputs; (b) A reference LCT map was developed from EBMC, map layers, and field data, to serve as the ground reference for evaluating the accuracy of automated classification results.

3.1. Development of LCT classification models

3.1.1. Classification models

Three clustering models were selected to present different paradigms in automated landscape classification. OPMC represents traditional multi-view clustering approaches that integrate expert knowledge through variable classification. SOFM represents neural network-based unsupervised learning methods with self-organising capabilities. Finally, STSC represents the latest deep learning approaches that combine unsupervised clustering with supervised spatial relationship learning. This selection provides comprehensive coverage of the major methodological approaches currently available for automated landscape classification, from established traditional methods to cutting-edge deep learning techniques. Despite the methodological differences, all three approaches are directly comparable as they begin with identical unlabelled input data and generate landscape classifications without human-provided labels. All cluster analyses were performed using MATLAB.

The **OPMC** algorithm processes all variables once through multiple expert-defined perspectives, making use of complementary information to improve clustering accuracy (Liu et al., 2021b). By integrating insights from different views, it outperforms single-view approaches in both robustness and precision. In this study, ten experts in landscape, geography, and land management classified variables as either "essential" or "non-essential" (Appendix C). During each iteration, the algorithm computed similarities or distances between data samples, assigned samples to the closest clusters, and updated cluster definitions. This process uncovered the underlying structure of the data more effectively. OPMC is particularly suitable for analysing large areas and

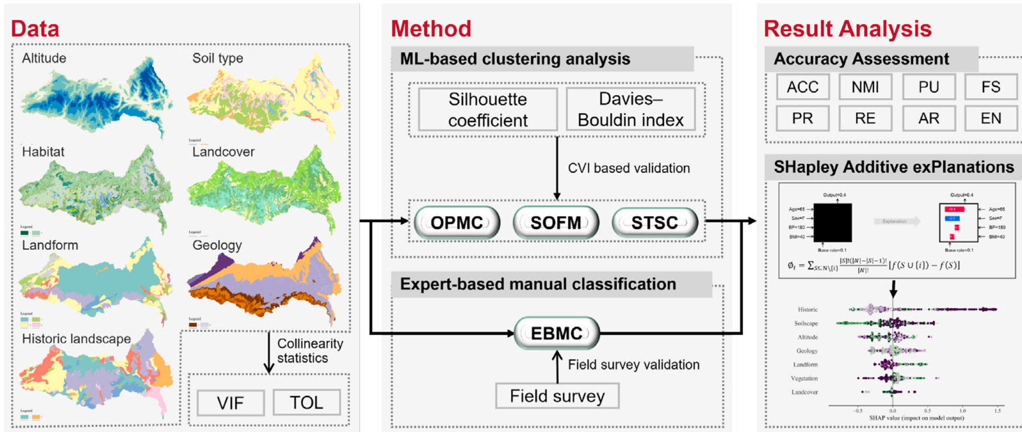

Fig. 2. Flowchart describing the main methodological steps and their sequence as applied in this research.

delivers stable, high-quality clustering results. The clustering process is guided by the following formula,

$$\min_{Y,\{C_v\}_{v=1}^{V},\{W_v\}_{v=1}^{V}} \frac{1}{V}\sum_{v=1}^{V}\|X_v - YC_vW_v\|_F^2$$
$$s.t.\quad W_vW_v^{\top} = I_k,\ y^{(i)} \in \{e_1, e_2, \dots, e_k\} \tag{2}$$

where $X^{(v)}$ is the vth view, Y_v is the hard partition matrix with each row being an orthonormal basis of k-dimension space. C_v is a centroid matrix and its jth row represents the jth centroid of H_v.

The **SOFM** is a neural network-based clustering algorithm that projects high-dimensional data into a lower-dimensional space through a process of self-organisation (Olga and Ross, 2020; Zhang et al., 2010). Unlike the centroid-based algorithm, SOFM relies on a competitive learning mechanism (Kohonen, 2013). During training, the network structure and weights automatically adjust to reflect the data distribution, with training ending once the clusters become clearly defined (Foody, 1999). SOFM is especially useful for handling complex and high-dimensional datasets. In this study, MATLAB's Neural Network Toolbox was used to implement SOFM. Parameters were set with a learning rate of 0.1 for the initial ordering phase and 0.02 for the fine-tuning phase. The training process included 5000 steps for ordering and 50,000 steps for tuning. The propagation and updating of weights in the SOFM follow the following computation process,

$$m_i(t+1) = m_i(t) + h_{ci}(t)[x(t) - m_i(t)] \tag{3}$$

where $h_{ci}(t)$ is the neighbourhood function, resembling the kernel applied in usual smoothing processes. The subscript c is the index of a particular node (winner) in the grid, namely, the model $m_c(t)$ with the smallest Euclidean distance from $x(t)$.

The **STSC** model combines K-means clustering with the Swin Transformer, a state-of-the-art deep learning architecture for image segmentation, representing a semi-supervised approach to landscape classification. In the first stage, K-means clustering groups the data into distinct clusters based on their features, creating initial pseudo-labels for landscape elements without requiring external ground truth annotations (Hartigan and Wong, 1979). In the second stage, these automatically generated pseudo-labels are used to train the Swin Transformer (Liu et al., 2021a; Huang et al., 2025a), enabling it to learn complex patterns and spatial relationships within the dataset through supervised learning techniques. This two-stage hybrid method is qualified as semi-supervised because it generates its own training labels from unlabelled data, allowing for efficient processing of large datasets while maintaining comparability with fully unsupervised methods. The mathematical formulation of this process is described as follows,

$$J = \sum_{i=1}^{n}\sum_{j=1}^{k} r_{ij}(x^i - \mu_j)^2 \tag{4}$$

where, j represents the sum of squared distances from each sample point to its centre of mass, k represents the number of clusters. μ_j denotes the category to which the 1st sample belongs, and r_{ij} is 1 when the data point x^i is classified to μ_j, and 0 otherwise.

In our study, the **EBMC** serves as the ground reference to compare the outcomes of automated classifications against, as it represents the established standard practice in LCA. The EMBC used in this study was conducted by co-author Steven Warnock following the standardised methodology (Warnock and Griffiths, 2015). This ensures methodological consistency and provides an authoritative reference against which automated methods can be reliably evaluated.

3.1.2. CVI-based clustering validation

Validating clustering results is essential in LCA, mainly because the number of clusters must be defined in advance. This is contradictory to unsupervised learning, where there is no clear "correct" number of clusters. Instead of focusing on exact labels, validation should assess whether the clustering meaningfully separates the data (Fraley and Raftery, 2002). In this study, we followed two key principles: keeping differences within each LCT as small as possible, and avoiding too many categories while still capturing important differences (Zhao et al., 2023). To evaluate model performance, we used the Clustering Validity Index, specifically the Silhouette Coefficient (SC) and Davies–Bouldin (DB) index.

The SC measures the average distance from sample i to other samples within the same cluster. It ranges from −1 to 1, with values closer to 1 indicating more compact and well-separated clusters, reflecting better clustering quality (Rousseeuw, 1987). In this analysis, SC is represented as follows,

$$SC = \frac{1}{N}\sum_{i=1}^{N}\frac{disMean_{out}(i) - disMean_{in}(i)}{\max\{disMean_{out}(i), disMean_{in}(i)\}} \tag{5}$$

where, $disMean_{in}$ is the average distance between the point and other points in the class, $disMean_{out}$ is the average distance between the point and non-class points, N is the total number of points clustered.

The DB index is used to assess the quality of clustering results, with lower values indicating better separation between clusters (Davies and Bouldin, 1979; Halkidi et al., 2001). It measures how similar each cluster is to the others, based on the distance between cluster centres and the spread of points within each cluster. A DB index close to zero means that clusters are compact and well-separated, which suggests a good clustering outcome. The formula for calculating the DB index is shown below,

$$DB = \frac{1}{K}\sum_{i,j=1}^{K}\max_{i\neq j}\left(\frac{\bar{d}_I + \bar{d}_J}{d_{i,j}}\right) \tag{6}$$

Table 2
Accuracy assessment metrics.

Definition	Metrics	Description
NMI is a measure used to evaluate network partitioning performed by community finding algorithms.	$NMI(X,Y) = \frac{2*I(X,Y)}{H(X)+H(Y)}$	where $I(X,Y)$ represents the mutual information between X and Y, while $H(X)$ and $H(Y)$ denote the entropy of X and Y respectively.
FS combines precision and recall in a single metric, the value of F-score ranges from 0 to 1, with closer to 1 indicating better model performance.	$FS = (1+\beta^2)\frac{PR \times RE}{\beta^2 PR+RE}$	where PR denotes the Precision value, RE represents the Recall value.
ACC is a metric used to evaluate the performance of classification models.	$ACC = \frac{TP+TN}{TP+FN+FP+TN}$	where TP (True Positive) refers to the number of pair of points that belong to the same clusters in both the true labels and the predicted labels; TN (True Negative) represents the number of samples correctly classified as negative; FP (False Positive) indicates the number of samples incorrectly classified as positive; and FN (False Negative) stands for the number of samples wrongly classified as negative.
PR measures the proportion of samples that are actually positive among all samples predicted as positive.	$PR = \frac{TP}{TP+FP}$	
RE reflects the proportion of samples that are actually positive and are predicted as positive by the model.	$RE = \frac{TP}{TP+FN}$	
ARI measures the similarity between the clustering result and the true labels; it adjusts Rand Index by randomly sampling the data.	$ARI = \frac{RI-E[RI]}{\max(RI)-E[RI]}$ $RI = \frac{TP+TN}{TP+FP+FN+TN}$	

where $\bar{d}_I$ is the average distance between each point in the ith cluster and the centroid of the ith cluster. $\bar{d}_J$ is the average distance between each point in the jth cluster and the centroid of the jth cluster. $d_{i,j}$ is the Euclidean distance between the centroids of the ith and jth clusters.

3.2. Explaining analysis

Although machine learning is known for its high accuracy and strong performance (Wang et al., 2020), it is often considered a "black box" approach due to a lack of information on how it makes decisions (Huang et al., 2024). The SHapley Additive Explanations (SHAP) method tackles this issue (Lundberg and Lee, 2017). Based on game theory, SHAP calculates how much each input feature (in our case, an LCE) contributes to the model's output, treating each feature as a player in a team. We used the SHAP analysis to measure the contribution of each LCE to the outputs of the three automated models and the reference classification. We plot the SHAP values for all elements across all samples to show which elements are most important for each model. The analysis is carried out using Python 3.7 with the shape library as follows,

$$\phi_i = \sum_{S \subseteq N \setminus \{i\}} \frac{|S|!(|N|-|S|-1)!}{|N|!}[f(S \cup \{i\}) - f(S)] \tag{7}$$

where, ϕ_i denotes the SHAP value for feature i, representing its contribution to the classification, N denotes the set of all features, S denotes a subset of N that does not include feature i, $f(S)$ denotes the model's classification when only the features in subset S are present.

3.3. Accuracy assessment

The quality of machine learning classification is often evaluated by how closely the model's results match the expected outcomes or known categories, often referred to as 'ground reference' (Halkidi et al., 2001). In this study, we use the EBMC map as the ground reference. We performed an accuracy assessment to test how well the models assign similar cells to the same cluster and separate different zones into distinct clusters.

Several evaluation metrics were applied: accuracy (ACC), normalised mutual information (NMI), precision (PR), recall (RE), F-score (FS), and adjusted rand index (ARI) (Halkidi et al., 2002). ACC shows how many samples were correctly classified. NMI measures the agreement between clustering and the ground reference. PR shows the proportion of correct positive predictions, while RE shows how many actual positives were correctly identified. FS combines PR and RE into one score. ARI adjusts for chance and considers both false positives and false negatives. The definitions of these six metrics are provided in Table 2. Each metric ranges from 0 to 1, with higher values indicating better clustering performance.

All geospatial data and analysis codes are publicly available through the BBNP_LCA GitHub repository. Custom MATLAB scripts for coordinate system unification are provided in the '/lib' directory.

4. Results

4.1. Cluster validation

In the CVI-based cluster validation, the optimal number of clusters (k) for each model was determined by identifying the point where the SC reached its maximum and the DB reached its minimum. Fig. 3 shows the average SC and DB values across five clustering and validation iterations for each model. Fig. 3(b) then shows that DB values decline sharply at first and then level off gradually. Since a higher SC (range [0,1]) and a lower DB (range $[0, \infty]$) indicate better clustering, the results suggest that the OPMC and KM models outperform SOFM in both metrics, particularly when k exceeds 8. Among the three models, OPMC consistently achieves the best clustering performance, with the highest SC (0.4410) and lowest DB (1.0712). The optimal number of clusters was found to be k = 16 for SOFM and k = 20 for both KM and OPMC.

4.2. Landscape character types generated by the four models

We applied the OPMC and SOFM models to perform clustering analysis on spatial data, resulting in 20 LCTs for OPMC and 16 LCTs for SOFM, as shown in Fig. 4(a–b). The STSC model, using K-means-generated pseudo-labels, produced 20 LCTs, displayed in Fig. 4(c). The EBMC identified 21 LCTs (Fig. 4(d). In Fig. 4(a–c), the LCT distributions appear more fragmented due to the pixel resolution of the input data. In contrast, Fig. 4(d) shows more cohesive LCTs with clearly defined boundaries drawn by experts. Despite methodological differences, all four models produce highly similar spatial patterns. For example, in the zoomed-in area 1, the ridge of Fan Brycheiniog is clearly delineated by all models; in area 2, the morphology of Pen y Fan is consistently captured; and in area 3, both the mountain and its surrounding lower slopes are accurately distinguished.

Fig. B.8 compares the area distribution of LCTs across the four models. The standard deviation analysis reveals that OPMC, SOFM, and STSC exhibit relatively uniform LCT areas, with STSC showing the most balanced distribution (standard deviation: 336.33 km^2). In the OPMC results (Fig. B.8(a)), types 10, 12, and 16 dominate, each exceeding 125

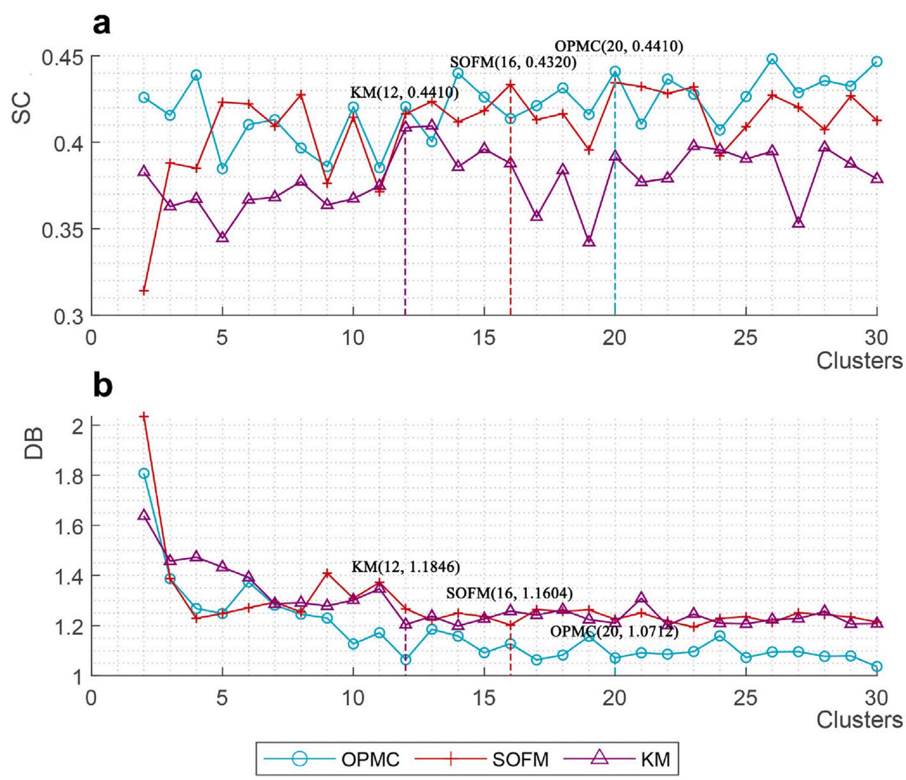

Fig. 3. Validation results for SC and DB: (a) SC validation; (b) DB validation. The best clustering results are obtained when the value of SC is at its highest and at the same time the value of DB is at its lowest. Combining the values of SC and DB, the best clustering results are obtained for OPMC when k = 20, SOFM when k = 16, and KM when k = 20.

km^2, while type 1 covers only 12.02 km^2. In SOFM (Fig. B.8(b), types 1 and 11 are largest, each around 175 km^2. In STSC (Fig. B.8(c)), types 2, 4, and 20 are most widespread, each over 125 km^2. In EBMC (Fig. B.8(d)), types 2 and 9 make up 44.3% of the total area, while type 17 is the smallest at 1.82 km^2.

We compared pixel-by-pixel classifications from our four models to explore how LCTs from each method align with one another. An extended Sankey plot generated using ChiPlot is shown in Fig. 5. Overall, the results show considerable consistency and clustering across models. For example, OPMC_LCT10, STSC_LCT20, EBMC_LCT2, and SOFM_LCT11 share similar geographic patterns, as do OPMC_LCT12, STSC_LCT4, EBMC_LCT9, and SOFM_LCT1.

The machine learning models — OPMC, STSC, and SOFM — show clearer clustering flows, while the EBMC results are more diverse, showing weaker and more dispersed flows. Notably, strong bidirectional correspondence is observed between OPMC and STSC. For instance, OPMC_LCT10 maps primarily to STSC_LCT20 (7.86%), and OPMC_LCT12 to STSC_LCT4 (8.07%). From STSC to EBMC, STSC_LCT4 maps to EBMC_LCT9 (5.44%) and STSC_LCT20 to EBMC_LCT2 (4.75%). Similarly, SOFM_LCT1 corresponds to EBMC_LCT9 (6.56%) and SOFM_LCT11 to EBMC_LCT2 (4.95%).

4.3. Contribution characteristics of LCEs based on SHapley Additive explanations

Fig. 6 presents the overall explanatory contribution of each LCE across the four classification models, SHAP to assess the importance of each element in shaping Landscape Character Types. The contribution rankings reveal distinct patterns: geology, historic landscape, and soil type consistently show higher contributions across all models, while habitat and landform contribute comparatively less in terms of SHAP value distribution relative to the centre (SHAP = 0). Both the OPMC and EBMC models display a balanced spread of contributions, with positive and negative values distributed on either side of the centre. The STSC model shows SHAP values predominantly on the right side of the centre, indicating strong and consistent positive contributions. The SOFM model, however, has SHAP values mostly to the left, suggesting more negative contributions and lower confidence in feature influence.

Fig. 6(a–c) show that the SHAP values for OPMC, SOFM, and STSC are more widely spread, indicating greater variability and uncertainty in feature dependency. Notably, the SOFM model shows weak dependence on features like soil type, possibly due to imbalanced training or less effective element selection. Meanwhile, OPMC and STSC demonstrate stronger and more consistent contributions from geology and landform, while also maintaining balanced contributions from historic landscape and soil type. In Fig. 6(d), representing the EBMC model, shows a more stable and concentrated SHAP value distribution. This likely reflects the consistency and prior knowledge used in manual classification, particularly for features such as geology and soil type. The relatively lower SHAP values for historic landscape and soil type suggest these features were considered less important in manual classification compared to automated models.

Fig. D.9 provides a focused comparison of the contributions of geology, historic landscape, and soil type across the four models. Geology emerges as the most influential element overall, with particularly high SHAP values in the OPMC and EBMC models, indicating that these models rely heavily on geological features for classification. Although geology is slightly less influential in the SOFM and STSC models, it still shows a notable impact. The importance of historic landscape varies more across models. OPMC and STSC assign relatively high SHAP values to this element, suggesting a stronger influence on their classification outcomes. In contrast, SOFM and EBMC display lower SHAP values for the historic landscape, indicating that it plays a lesser role in those models. While historic landscape generally contributes less than geology, its role is more pronounced in the OPMC and STSC models.

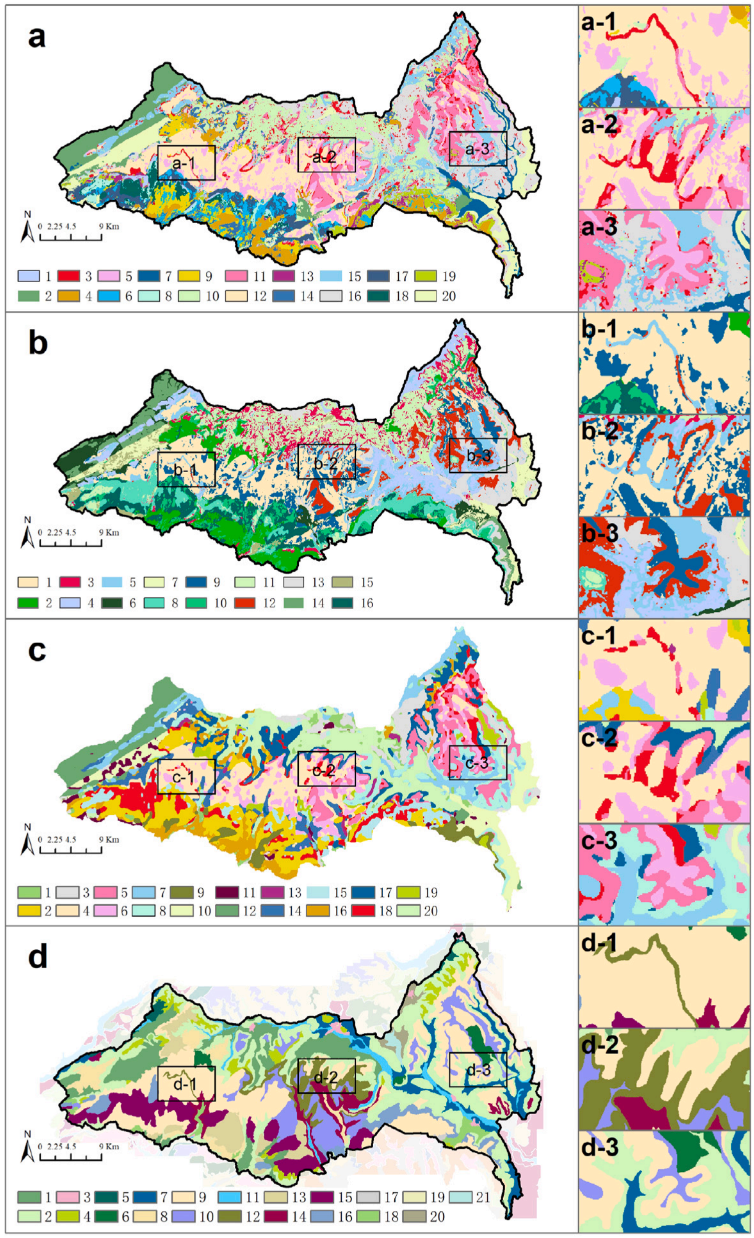

Fig. 4. Visual comparison of landscape character classification results across automated and expert-based methods. (a) OPMC Results (b) SOFM Results (c) STSC Results (d) EBMC (Expert) Results. Inset areas: 1-Fan Brycheiniog, 2-Pen y Fan, 3-East BBNP.

4.4. Similarity measurement

Fig. 7 shows the results of the accuracy assessment of OPMC, SOFM, and STSC models against the EBMC. Higher values across these metrics indicate better alignment with the EBMC results. All three models — OPMC, SOFM, and STSC — achieved high scores for ACC, NMI, FS, PR, and AR, with ACC and NMI values nearing 0.85, suggesting strong overall consistency. However, notable variation was observed in PR and RE values, particularly in the SOFM model, which displayed an inverse trend compared to OPMC and STSC.

Overall, the OPMC and STSC models outperformed SOFM across all six evaluation metrics. STSC stood out in particular, achieving the highest scores for Accuracy (0.845), Normalised Mutual Information (0.974), and Recall (0.947), indicating strong agreement with the expert-based classification. While OPMC performed best in terms of Precision, it scored lower in Recall. SOFM delivered more balanced results overall but ranked slightly lower than the other two models in most metrics. In conclusion, STSC is the most consistent model and is well-suited for applications requiring balanced performance, whereas OPMC may be preferred when higher precision is the main priority.

4.5. Landscape interpretation of dominant cluster types

To address the landscape meaning of data-driven clusters, we conducted detailed environmental composition analysis for each automated cluster type. Through pixel-by-pixel percentage analysis, we obtained the distribution characteristics of all 60 environmental variables (Appendix A) for each cluster type across the three automated methods.

The automated clusters exhibit coherent environmental signatures that correspond to recognisable landscape types. Clusters dominated by specific geological substrates, elevation ranges, and soil types consistently co-occur with particular vegetation patterns and historic land use signatures, creating environmentally coherent landscape units.

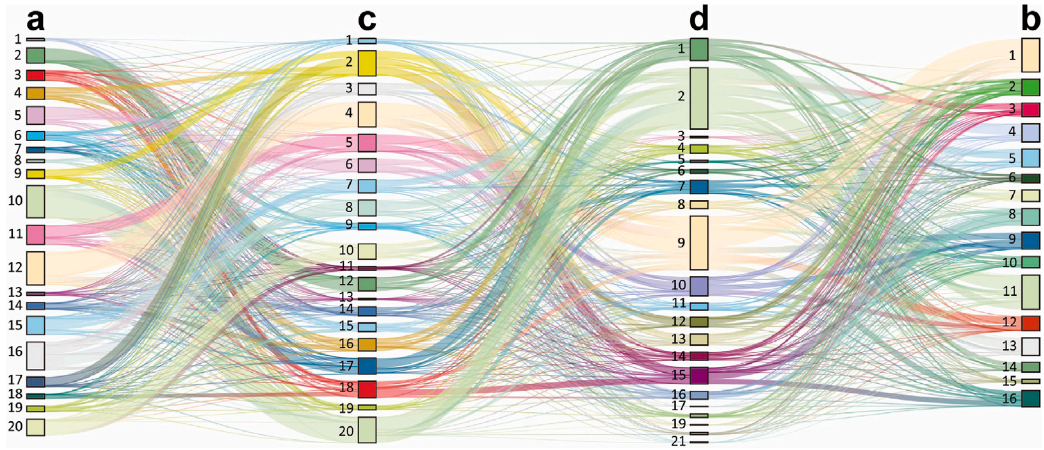

Fig. 5. Mutual flow relationships for LCT results from the four models: (a) OPMC; (b) SOFM; (c) STSC; (d) EBMC. The nodes in each column correspond to the LCTs, with their height indicating the area occupied by each type. Different colours represent the flows between various designated types, while the width indicates their magnitude.

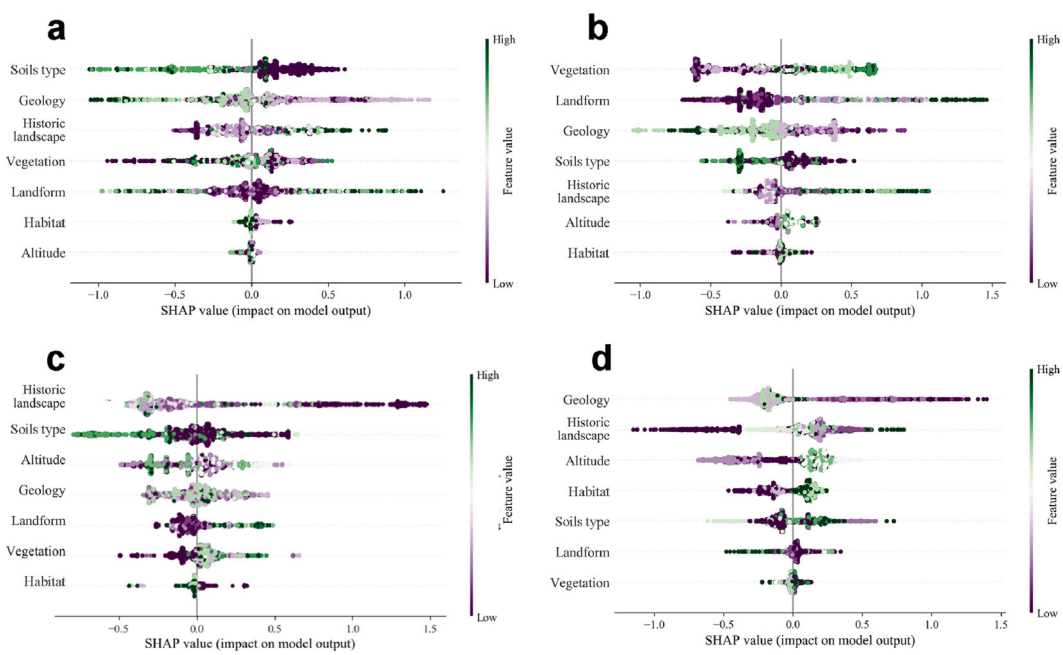

Fig. 6. Beeswarm plots of global interpretability for four models: (a) OPMC; (b) SOFM; (c) STSC; (d) EBMC. Each row of the graph represents an element and is sorted by the average absolute value of SHAP. A point in the graph represents a sample, with the greener colour representing a greater element contribution and the purple colour representing a lesser element contribution.

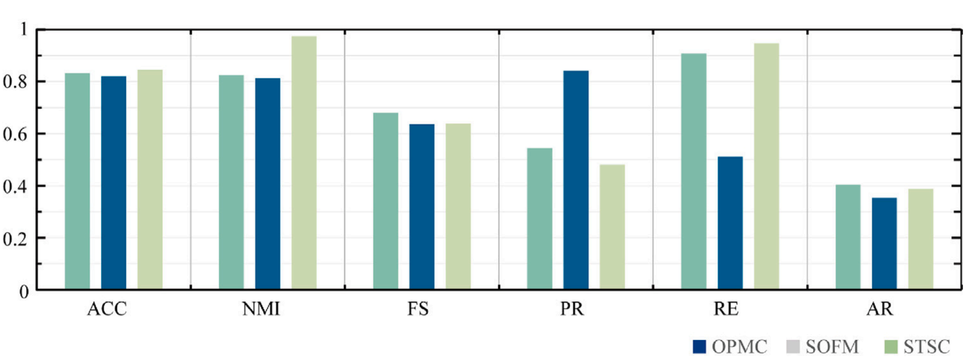

Fig. 7. Results of accuracy assessment for OPMC, SOFM, and STSC with EBMC, respectively.

Table 3
Comparison of landscape character type descriptions between automated and expert classifications.

Automated type	Key variable composition	Expert type	Expert description
STSC_LCT20	61.3% elevation 250–350 m + 68% Devonian Argillaceous Rock + 78% Prehistoric-Medieval historic landscape + 65% Cultivated Terrestrial Vegetation + 94% Dissected lowland plateau + 92.5% Freely draining acid loamy soils + 57.7% Improved Grassland.	EBMC_LCT2: Wooded Hills & Slopes	Gently rolling hills on argillaceous geology with well-drained soils supporting improved grasslands. Historic field patterns reflect centuries of pastoral farming with scattered woodland remnants.
STSC_LCT4	58.2% elevation 450–600 m + 96.9% Devonian Sandstone + 71.2% Prehistoric-Medieval historic landscape + 47.9% Semi-natural Terrestrial herbaceous vegetation + 50.8% wet acid upland soils + 78.6% moor grassland.	EBMC_LCT9: Moorland Hills & Slopes	Higher elevation landscapes on sandstone geology with acidic, poorly-drained soils supporting semi-natural moorland vegetation. Extensive grazing systems with minimal settlement.

The Mutual flow analysis (Fig. 4) demonstrates strong bidirectional correspondence between automated and expert classifications, with key correspondences including STSC_LCT20 - EBMC_LCT2 (4.75%) and STSC_LCT4 - EBMC_LCT9 (5.44%).

Based on environmental composition analysis and expert correspondence, the dominant automated cluster types can be characterised as meaningful landscape units (Table 3). For example, STSC_LCT20 represents mid-elevation pastoral landscapes characterised by 61.3% elevation 250–350 m, 68% Devonian Argillaceous Rock geology, and 92.5% freely draining acid loamy soils supporting improved grasslands. This corresponds closely to EBMC_LCT2 "Wooded Hills & Slopes", described as pastoral landscapes with well-drained soils and historic field patterns. Similarly, STSC_LCT4 represents upland moorland systems with 58.2% elevation 450–600 m, 96.9% Devonian Sandstone geology, and 78.6% moor grassland, corresponding to EBMC_LCT9 "Moorland Hills & Slopes".

The environmental composition analysis reveals that automated clusters represent landscape units with similar environmental characteristics and management requirements. These findings demonstrate that data-driven clustering produces meaningful landscape types with clear environmental coherence, addressing concerns about clusters lacking landscape significance. The strong correspondence with expert classification validates that automated methods can identify environmentally coherent landscape units that serve as valuable foundations for landscape character assessment.

5. Discussion

5.1. Landscape characterisation

This research compares LCT classifications using machine learning, deep learning, and expert-based methods. A fundamental theoretical question in automated landscape character assessment concerns whether data-driven clustering can produce meaningful landscape types beyond statistical artifacts. Our environmental composition analysis addresses this challenge by demonstrating that automated methods identify the underlying biophysical template that supports landscape character formation. While traditional LCA emphasises perceptual and experiential dimensions, our findings show that objective environmental patterns can capture the essential landscape-forming processes that underpin these perceptual characteristics.

The strong correspondence between automated clusters and expert-recognised landscape types (Table 3) validates this approach. For instance, STSC_LCT20's environmental signature — characterised by mid-elevation pastoral landscapes on well-drained soils — directly corresponds to the expert-identified "Wooded Hills & Slopes" character type. This consistency between automated and expert classifications suggests that data-driven methods can successfully identify meaningful landscape units with clear environmental coherence and management relevance, rather than producing arbitrary statistical clusters.

However, a significant practical challenge remains in the interpretability and accessibility of automated classifications. Manual classification generates intuitive, easily recognisable labels such as 'grassland', 'forest', or 'urban area', immediately understandable by a wide audience. These labels stem directly from expert interpretation and experiential knowledge. In contrast, automated methods typically produce less intuitive labels such as 'Class19' or 'Cluster3', which lack immediate clarity and make it challenging for practitioners, policymakers, or stakeholders to use them effectively (Fagerholm et al., 2013). Therefore, bridging the gap between the environmental accuracy of automated classifications and the intuitive accessibility of expert-derived labels remains essential for improving both the precision and practical usability of landscape assessments.

5.2. Implications of automated classification for landscape character identification

Reducing subjectivity in landscape classification is a major goal in LCA. At its core, LCA seeks to establish a robust baseline framework that subdivides study areas into landscape types sharing similar natural and cultural attributes, providing consistent spatial units for subsequent landscape analysis and monitoring activities (Simensen et al., 2018). This study demonstrates that automated methods, particularly those involving machine and deep learning, are effective tools for establishing the baseline LCT framework objectively.

Automated clustering analyses group landscape samples based on similarities in their natural and cultural elements, significantly reducing researcher bias and providing the consistency necessary for reliable baseline establishment (Huang et al., 2023). Previous research also supports this, showing that automated methods can systematically integrate multiple landscape elements to produce consistent and objective classifications suitable for creating stable spatial frameworks (Myadzelets, 2021; Simensen et al., 2018; Huang et al., 2023). Our comparative analysis of three automated classification methods (OPMC, SOFM, and STSC) found that their results were largely consistent with one another, with accuracy assessment against EBMC highlighting that the STSC model most closely matched expert-driven classifications.

The findings highlight several key advantages of using automated methods for establishing landscape character baselines. Firstly, they significantly reduce the time required for classifying landscape types and delineating their boundaries compared to traditional manual approaches, enabling baseline establishment at previously impractical scales. For instance, while a comprehensive manual LCA for large regions can require decades of expert work, automated methods can establish similar frameworks within a fraction of that timeframe. Secondly, automated methods do not require the number of landscape types to be predefined, allowing for data-driven determination of natural landscape divisions. Most importantly, automated methods enhance objectivity and repeatability, providing consistent baseline frameworks that can serve as reliable spatial units for conservation planning, environmental impact assessment, and landscape management decisions.

This systematic consistency means that automated classification methods can be replicated across different geographic areas (Huang et al., 2025b), making them particularly valuable for creating standardised landscape character frameworks that support evidence-based policy development. The scalability demonstrated by our methods addresses the fundamental challenge where the need for comprehensive landscape characterisation far exceeds the capacity of traditional expert-based approaches, particularly in regions lacking established LCA programs. While our study focuses on methodological comparison, these advances provide essential foundations for enabling LCA applications at regional and national scales where landscape character frameworks are critically needed for sustainable development and conservation planning.

5.3. Migratory and global perspectives on automatic classification methods

Automated landscape character classification methods, like those applied to Bannau Brycheiniog National Park in this study, have significant potential for broader global applications due to the increasing availability of remote sensing data. Global Earth observation programs, such as the European Space Agency's Copernicus and NASA's Earth Observing System, now provide extensive satellite data that support large-scale landscape analysis. The rise of open-access data platforms further promotes information sharing and allows landscape character assessments to extend beyond local or national boundaries, enabling comparative studies across continents (Wascher, 2005). This enhanced global accessibility means that methods initially tested at smaller scales can be effectively adapted and expanded to larger and more diverse regions.

The scalability of automated classification is further strengthened through standardised approaches and unified analytical frameworks. Methods like unsupervised clustering algorithms (e.g., OPMC, SOFM) and semi-supervised deep learning techniques (e.g., STSC) offer consistency in identifying landscape types across varied geographical areas (Yang et al., 2020). Standardisation simplifies the adaptation of these methods to new regions and enhances the comparability of results. When classification methods are consistent and unified, findings from one landscape can be reliably applied or compared to others. Employing common evaluation metrics, such as the Clustering Validity Index, further ensures uniformity, making landscape assessments easier to replicate and analyse across different ecosystems (Alfredsen et al., 2022; Huang et al., 2023). Such consistency is critical for efficient environmental monitoring and informed policy-making at regional, national, and global levels.

Additionally, as landscapes change in response to climate change, human activities, and migratory species, monitoring these shifts becomes increasingly important (Turner, 2010). Automated methods, with their inherent scalability and adaptability, enable long-term observation of landscape dynamics. For example, researchers can track changes in vegetation or soil type patterns caused by migratory species and other environmental factors consistently across multiple regions. This temporal monitoring capability is especially valuable for biodiversity conservation and sustainable management. By adopting standardised, scalable automated classification methods, landscape changes can be studied effectively over time, providing essential data for both local and global conservation strategies. Consequently, this standardised approach facilitates a more comprehensive understanding of landscape evolution and supports global efforts to manage landscapes sustainably in a rapidly changing world (Yang et al., 2020; Griffiths, 2018).

5.4. Limitations and future work

This study demonstrated the comparative effectiveness of automated methods for identifying LCTs within Bannau Brycheiniog National Park. However, several limitations remain, pointing to important areas for future research and methodological refinement.

The most significant limitation concerns the geographic scope and generalisability of our findings. Our validation relies exclusively on expert classification within BBNP, a specific upland Welsh landscape context characterised by particular geological, topographical, and cultural attributes. While this focused approach ensured high-quality ground truth data and demonstrated clear methodological effectiveness within our study area, it raises important questions about model transferability across different landscape settings. The relationships between automated methods that we observed may not hold in regions with contrasting topographies, land use patterns, or cultural attributes. Cross-site validation using other protected areas from the UK National Parks system (Fig. 1) — such as lowland agricultural areas (Norfolk Broads), coastal environments (Pembrokeshire Coast), or different geological contexts (Lake District) — would provide essential insights into model robustness and help identify which landscape characteristics most strongly influence classification performance. Such external validation would enable the development of adaptive strategies for applying automated LCA methods across diverse environmental contexts, ultimately supporting broader adoption of these approaches in landscape management.

A second methodological challenge involves the covariance among landscape character elements. High collinearity between variables can obscure distinctions between landscape types and influence classification model performance, particularly when scaling across different geographic contexts. Future studies should explore multiscale or hierarchical modelling approaches, alongside dimensionality reduction techniques such as Principal Component Analysis, to reduce redundancy and improve the interpretability of classification outputs across diverse landscape settings.

The temporal dimension represents another important limitation. This study focuses on single-time-point classification without assessing the temporal stability of automated methods. Evaluating whether these techniques can produce consistent results over time is critical for supporting long-term landscape monitoring and establishing robust baseline assessments, particularly as landscapes respond to climate change and human pressures.

6. Conclusions

This study demonstrates that automated classification methods — OPMC, SOFM, and STSC — can effectively generate LCTs with greater scalability and repeatability than the traditional expert-based approach. Among the three methods, STSC showed the strongest agreement with the expert-based reference, highlighting its potential for high-quality landscape characterisation.

Importantly, the automated LCTs produced through this study provide a reliable spatial foundation for monitoring key ecological and environmental variables such as land use and land cover changes, habitat dynamics, fire frequency, carbon storage, and species distributions. These are essential components for managing landscape responses to habitat degradation, biodiversity loss, and the broader impacts of climate change on food and ecosystem security.

While the performance of automated methods is promising, some limitations remain, notably the generation of character types interpretable by stakeholders. Future research should focus on integrating automated methods with expert knowledge to enhance both the interpretability and credibility of classification outputs. Such hybrid approaches would ensure that automated LCA frameworks are not only scientifically robust but also practical for supporting diverse monitoring, planning, and management applications across a wide range of environmental contexts.

Table A.4
Landscape character elements.

ID	Variables	%	ID	Variables	%
Altitude/m			l8	Tectonically controlled topography	0.84%
al1	80–250	17.64%	l9	Undulating lowland hill terrain	2.99%
al2	250–350	24.74%	l10	Undulating upland terrain and dissected plateau	0.92%
al3	350–450	25.06%	l11	Upland and mountain river and stream	1.38%
al4	450–600	23.73%	l12	Upland glacial and fluvioglacial depositional terrain	0.23%
al5	600–931	8.83%	**Vegetation**		
Geology			v1	Natural terrestrial vegetation	0.43%
g1	Carboniferous: limestone	6.00%	v2	Moor grassland	28.73%
g2	Carboniferous: mudstone	6.97%	v3	Coniferous woodland	6.79%
g3	Carboniferous: sandstone	9.43%	v4	Broadleaf woodland	15.61%
g4	Carboniferous: argillaceous rock	27.19%	v5	Limestone grassland	3.23%
g5	Devonian: conglomerate	0.16%	v6	Improved grassland	24.27%
g6	Devonian: mudstone	0.67%	v7	Heathland	12.72%
g7	Devonian: sandstone	41.00%	v8	Bog	4.54%
g8	Ordovician	1.11%	v9	Cultivated	3.68%
g9	Silurian: quartzite	0.07%	**Habitat**		
g10	Silurian: else	7.41%	ha1	Cultivated terrestrial vegetation	27.03%
Soil type			ha2	Semi-natural terrestrial woody vegetation	17.26%
s1	Blanket bog peat soils	2.40%	ha3	Semi-natural terrestrial herbaceous vegetation	28.63%
s2	Freely draining acid loamy soils	53.55%	ha4	Natural aquatic vegetation	23.68%
s3	Freely draining floodplain soils	2.34%	ha5	Artificial surface	1.47%
s4	Restored soils mostly from quarry and opencast spoil	0.52%	ha6	Bare surface	0.19%
s5	Slightly acid loamy and clayey soils with impeded drainage	6.49%	ha7	Water	1.75%
s6	Slowly permeable wet very acid upland soils with a peaty surface	23.55%	**Historic landscape**		
s7	Unclassified	10.56%	hl1	Prehistoric, Roman, medieval, post medieval	15.82%
s8	Water	0.59%	hl2	Prehistoric, Roman, post medieval	16.44%
Landform			hl3	Prehistoric, medieval, post medieval, later period	28.51%
l1	Dissected lowland plateau	50.09%	hl4	Prehistoric, medieval, post medieval	14.92%
l2	Glaciated mountain terrain	20.23%	hl5	Prehistoric, post medieval, industrial, recent	8.31%
l3	Karst	10.46%	hl6	Roman, medieval, post medieval	7.37%
l4	Lowland glacial and fluvioglacial depositional terrain	4.14%	hl7	Medieval, post medieval, industria	1.83%
l5	Lowland river and drainage systems	2.48%	hl8	Post medieval, industrial, recent	5.87%
l6	Lowland scarp and dip-slope dominated terrain	0.70%	hl9	Industrial, recent	0.93%
l7	Man-made	5.53%			

Table C.5
Ten experts expressed 10 opinions on whether landscape character elements (LCE) are involved in the landscape classification process.

Multi-view	Altitude	Soil type	Geology	Landform	Vegetation	Historic landscape	Habitat
V1[a]	1[b]	1	1	1	1	1	1
V2	1	1	1	1	1	1	0
V3	1	1	0	0	1	1	1
V4	1	1	1	1	1	1	1
V5	0	1	0	1	1	1	1
V6	1	1	1	1	1	0	0
V7	1	1	1	1	1	1	1
V8	1	0	0	1	1	1	1
V9	1	1	0	0	1	1	0
V10	1	1	1	1	1	0	1

[a] Multi-views form 10 experts;
[b] 1 denotes "essential", 0 denotes "not essential".

CRediT authorship contribution statement

Tingting Huang: Writing – original draft, Visualization, Software, Methodology, Investigation, Funding acquisition, Formal analysis, Data curation, Conceptualization. **Geoffrey Griffiths:** Writing – review & editing, Validation, Project administration, Investigation, Conceptualization. **Bo Huang:** Software, Methodology, Funding acquisition. **Jianning Zhu:** Writing – review & editing, Supervision. **Steven Warnock:** Validation, Investigation. **Martin Lukac:** Writing – review & editing, Validation, Supervision, Project administration.

Declaration of competing interest

The authors declare that they have no known competing financial interests or personal relationships that could have appeared to influence the work reported in this paper.

Acknowledgements

This study is funded by the China Scholarship Council (No. 202206510014), the National Natural Science Foundation of China (No. 62306049 and No. W2421089), the General Program of Chongqing Natural Science Foundation (No. CSTB2023NSCQ-MSX0665), and the Fundamental Research Funds for the Central Universities, China (No. 2024CDJXY008). We thank the British Geology Survey (BGS) for the licence to use the onshore digital geological map of Great Britain data (1:50000).

Appendix A. Landscape character elements

Table A.4 shows the 60 variables from seven elements.

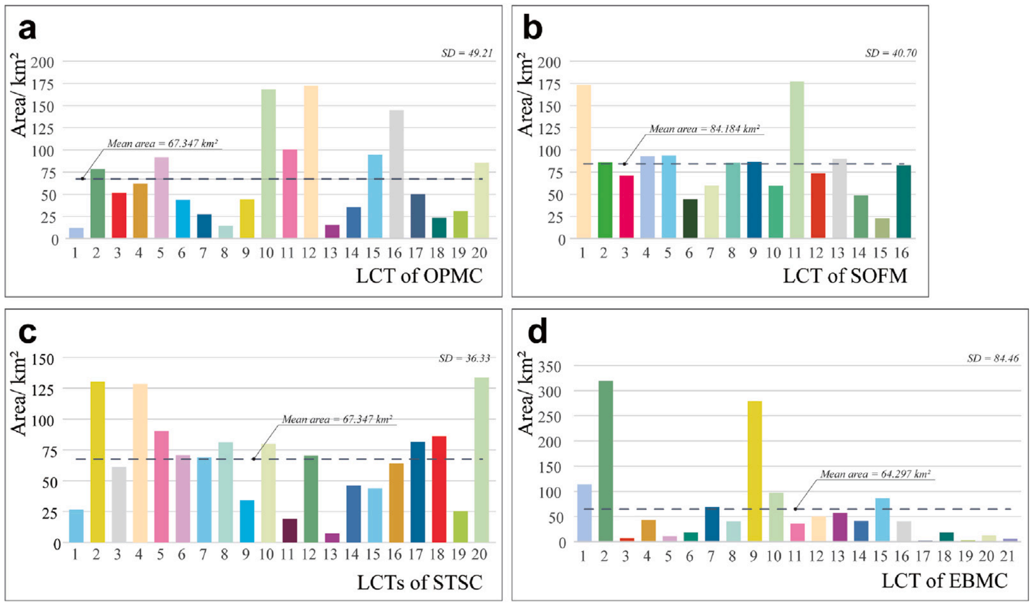

Fig. B.8. Area comparison of four models. (a) OPMC; (b) SOFM; (c) STSC; (d) EBMC. The rows represent the numbers of the LCTs, and the columns represent the size of the area of each type.

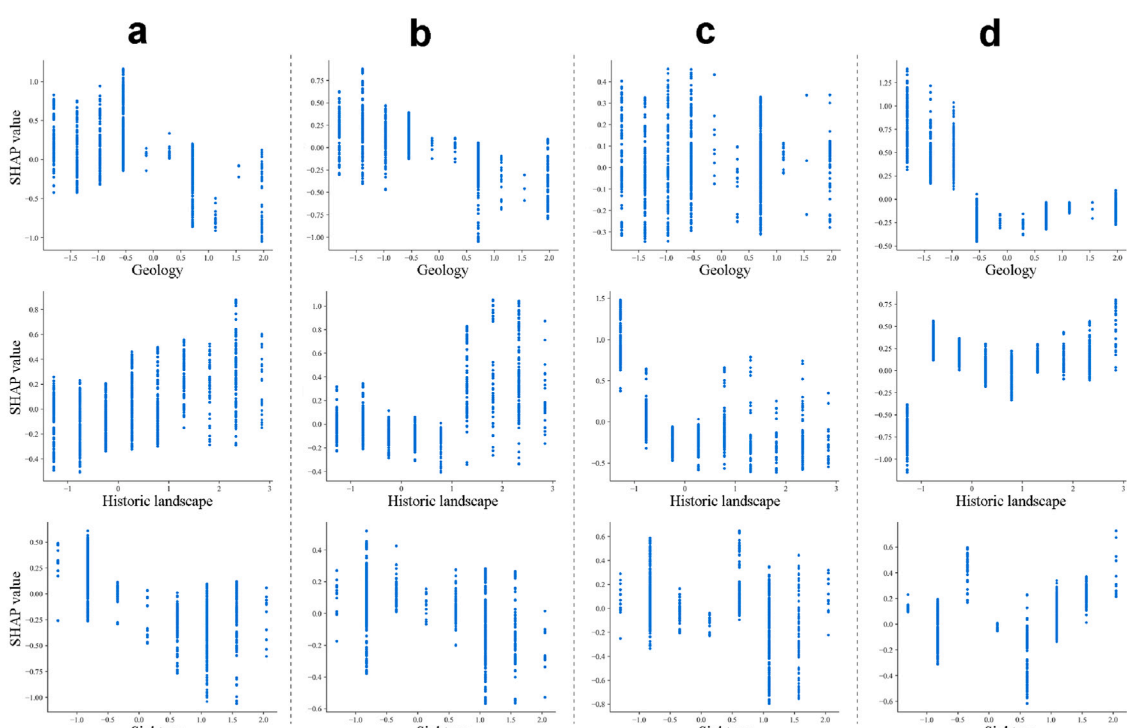

Fig. D.9. Scatter Plots of the geology, historic and soil type for four models: (a) OPMC; (b) SOFM; (c) STSC; (d) EBMC. The horizontal axis represents the actual value of the feature and the vertical axis represents the corresponding SHAP value.

Appendix B. OPMC, SOFM, STSC, and EBMC model clustering results

The area comparison of OPMC, SOFM, STSC, and EBMC model clustering results is demonstrated in Fig. B.8.

Appendix C. Multi-views from experts

Ten experts expressed 10 opinions on whether landscape character elements (LCE) are involved in the landscape classification process, the multi-view results are presented in Table C.5.

Appendix D. Scatter Plots of the geology, historic landscape and soil type for four models

Scatter Plots of the geology, historic landscape and soil type for four models are presented in Fig. D.9

Data availability

All data and code used in this study are publicly available at GitHub (https://github.com/TingtingHwang/BBNP_LCA). The repository includes raw data, processed datasets, analysis scripts, and detailed documentation for complete reproduction of results.

References

Alfredsen, K., Dalsgård, A., Shamsaliei, S., Halleraker, J.H., Gundersen, O.E., 2022. Towards an automatic characterization of riverscape development by deep learning. River Res. Appl. 38 (4), 810–816.

2010. Dataset: ©JAXA/METI alos PALSAR L1.0 2006 [dataset]. http://dx.doi.org/10.5067/J4JVCFDDPEW1, Accessed through ASF DAAC 25 November 2023.

Amani, M., Foroughnia, F., Moghimi, A., Mahdavi, S., Jin, S., 2023. Three-dimensional mapping of habitats using remote-sensing data and machine-learning algorithms. Remote. Sens. 15 (17), http://dx.doi.org/10.3390/rs15174135.

Antrop, M., Van Eetvelde, V., 2000. Holistic aspects of suburban landscapes: visual image interpretation and landscape metrics. Landsc. Urban Plan. 50 (1), 43–58. http://dx.doi.org/10.1016/S0169-2046(00)00079-7.

2023. British Geological Survey. (2023). BGS Geology 50K [Dataset]. British Geological Survey, URL: https://www.bgs.ac.uk/datasets/bgs-geology-50k-digmapgb/.

Brabyn, L., 2009. Classifying landscape character. Landsc. Res. 34 (3), 299–321. http://dx.doi.org/10.1080/01426390802371202.

Brown, G., Brabyn, L., 2012. An analysis of the relationships between multiple values and physical landscapes at a regional scale using public participation GIS and landscape character classification. Landsc. Urban Plan. 107 (3), 317–331. http://dx.doi.org/10.1016/j.landurbplan.2012.06.007.

Buller, H., Furuseth, O., Gilg, A.W., Lapping, M., 2012. Sustainable Rural Systems: Sustainable Agriculture and Rural Communities. Ashgate Publishing, Ltd..

Capotorti, G., Guida, D., Siervo, V., Smiraglia, D., Blasi, C., 2012. Ecological classification of land and conservation of biodiversity at the national level: The case of Italy. Biol. Cons. 147 (1), 174–183. http://dx.doi.org/10.1016/j.biocon.2011.12.028.

Carvalho, D.V., Pereira, E.M., Cardoso, J.S., 2019. Machine learning interpretability: A survey on methods and metrics. Electron. 8 (8), http://dx.doi.org/10.3390/electronics8080832.

Collier, D., LaPorte, J., Seawright, J., 2012. Putting typologies to work: Concept formation, measurement, and analytic rigor. Political Res. Q. 65 (1), 217–232. http://dx.doi.org/10.1177/1065912912437162.

Cui, Y., Yang, G., Zhou, Y., Zhao, C., Pan, Y., Sun, Q., Gu, X., 2023. AGTML: A novel approach to land cover classification by integrating automatic generation of training samples and machine learning algorithms on Google Earth Engine. Ecol. Indic. 154, 110904. http://dx.doi.org/10.1016/j.ecolind.2023.110904.

Davies, D.L., Bouldin, D.W., 1979. A cluster separation measure. IEEE Trans. Pattern Anal. Mach. Intell. PAMI-1 (2), 224–227. http://dx.doi.org/10.1109/TPAMI.1979.4766909.

Déjeant-Pons, M., 2006. The European landscape convention. Landsc. Res. 31 (4), 363–384. http://dx.doi.org/10.1080/01426390601004343.

Fagerholm, N., Käyhkö, N., Van Eetvelde, V., 2013. Landscape characterization integrating expert and local spatial knowledge of land and forest resources. Environ. Manag. 52, 660–682. http://dx.doi.org/10.1007/s00267-013-0121-x.

Fairclough, G., Herlin, I.S., Swanwick, C., 2018. Routledge Handbook of Landscape Character Assessment: Current Approaches to Characterisation and Assessment. Routledge, London, pp. 392–393. http://dx.doi.org/10.4324/9781315753423.

Fairclough, G., Herring, P., 2016. Lens, mirror, window: interactions between historic landscape characterisation and landscape character assessment. Landsc. Res. 41 (2), 186–198. http://dx.doi.org/10.1080/01426397.2015.1135318.

Foody, G.M., 1999. Applications of the self-organising feature map neural network in community data analysis. Ecol. Model. 120 (2), 97–107. http://dx.doi.org/10.1016/S0304-3800(99)00094-0.

Fraley, C., Raftery, A.E., 2002. Model-based clustering, discriminant analysis, and density estimation. J. Amer. Statist. Assoc. 97 (458), 611–631. http://dx.doi.org/10.1198/016214502760047131.

Griffiths, G., 2018. Transferring landscape character assessment from the UK to the Eastern Mediterranean: Challenges and perspectives. Land 7 (1), http://dx.doi.org/10.3390/land7010036.

Halkidi, M., Batistakis, Y., Vazirgiannis, M., 2001. On clustering validation techniques. Journal of intelligent information systems. J. Intell. Inf. Syst. 17, 107–145. http://dx.doi.org/10.1023/A:1012801612483.

Halkidi, M., Batistakis, Y., Vazirgiannis, M., 2002. Cluster validity methods: part I. SIGMOD Rec. 31 (2), 40–45. http://dx.doi.org/10.1145/565117.565124.

Hartigan, J.A., Wong, M.A., 1979. Algorithm AS 136: A K-means clustering algorithm. J. R. Stat. Soc. Ser. C (Appl. Stat.) 28 (1), 100–108, URL: http://www.jstor.org/stable/2346830.

Huang, T., Huang, B., Li, S., Zhao, H., Yang, X., Zhu, J., 2025a. SwinClustering: a new paradigm for landscape character assessment through visual segmentation. Front. Environ. Sci. Volume 13 - 2025, http://dx.doi.org/10.3389/fenvs.2025.1509113, URL: https://www.frontiersin.org/journals/environmental-science/articles/10.3389/fenvs.2025.1509113.

Huang, F., Jiang, S., Li, L., Zhang, Y., Zhang, Y., Zhang, R., Li, Q., Li, D., Shangguan, W., Dai, Y., 2024. Applications of explainable artificial intelligence in earth system science. http://dx.doi.org/10.48550/arXiv.2406.11882, arXiv preprint arXiv:2406.11882.

Huang, T., Zhang, Y., Li, S., Griffiths, G., Lukac, M., Zhao, H., Yang, X., Wang, J., Liu, W., Zhu, J., 2023. Harnessing machine learning for landscape character management in a shallow relief region of China. Landsc. Res. 48 (8), 1019–1040. http://dx.doi.org/10.1080/01426397.2023.2241390.

Huang, T., Zhao, H., Huang, B., Li, S., Zhu, J., 2025b. Integrating natural language processing with vision transformer for landscape character identification. IEEE J. Sel. Top. Appl. Earth Obs. Remote. Sens. 18, 5838–5852. http://dx.doi.org/10.1109/JSTARS.2025.3538174.

James, G., Witten, D., Hastie, T., Tibshirani, R., Taylor, J., 2013. An introduction to statistical learning. http://dx.doi.org/10.1201/9781315120256.

Kohonen, T., 2013. Essentials of the self-organizing map. Neural Netw. 37, 52–65. http://dx.doi.org/10.1016/j.neunet.2012.09.018, Twenty-fifth Anniversary Commemorative Issue.

Li, T., Johansen, K., McCabe, M.F., 2022. A machine learning approach for identifying and delineating agricultural fields and their multi-temporal dynamics using three decades of Landsat data. ISPRS J. Photogramm. Remote Sens. 186, 83–101. http://dx.doi.org/10.1016/j.isprsjprs.2022.02.002.

Liu, Z., Lin, Y., Cao, Y., Hu, H., Wei, Y., Zhang, Z., Lin, S., Guo, B., 2021a. Swin transformer: Hierarchical vision transformer using shifted windows. In: Proceedings of the IEEE/CVF International Conference on Computer Vision. ICCV, pp. 10012–10022.

Liu, J., Liu, X., Yang, Y., Liu, L., Wang, S., Liang, W., Shi, J., 2021b. One-pass multi-view clustering for large-scale data. In: Proceedings of the IEEE/CVF International Conference on Computer Vision. ICCV, pp. 12344–12353.

Lundberg, S.M., Lee, S.-I., 2017. A unified approach to interpreting model predictions. In: Proceedings of the 31st International Conference on Neural Information Processing Systems. NIPS '17, Curran Associates Inc., Red Hook, NY, USA, pp. 4768–4777.

Mücher, C., Bunce, R., Jongman, R., Klijn, J., Koomen, A., Metzger, M., Wascher, D., 2003. Identification and characterisation of environments and landscapes in europe. Technical Report, Alterra.

Mücher, C.A., Klijn, J.A., Wascher, D.M., Schaminée, J.H., 2010. A new European Landscape Classification (LANMAP): A transparent, flexible and user-oriented methodology to distinguish landscapes. Ecol. Indic. 10 (1), 87–103. http://dx.doi.org/10.1016/j.ecolind.2009.03.018, Landscape Assessment for Sustainable Planning.

Myadzelets, A., 2021. Mapping the pyrogenic dynamics of forest geosystems on the northeastern shore of Lake Baikal. In: IOP Conference Series: Earth and Environmental Science. Vol. 895, IOP Publishing, 012032. http://dx.doi.org/10.1088/1755-1315/895/1/012032.

Myers, R.H., 1990. Classical and Modern Regression with Applications, vol. 2, Duxbury press Belmont, CA.

Olga, K., Ross, S.P., 2020. From online texts to landscape character assessment: Collecting and analysing first-person landscape perception computationally. Landsc. Urban Plan. 197, 103757. http://dx.doi.org/10.1016/j.landurbplan.2020.103757.

Owers, C., Lucas, R., Clewley, D., Planque, C., Punalekar, S., Tissott, B., Chua, S., Bunting, P., Mueller, N., Metternicht, G., 2021. Big earth data 5, 368–390 [dataset]. http://dx.doi.org/10.1080/20964471.2021.1948179.

Rousseeuw, P.J., 1987. Silhouettes: A graphical aid to the interpretation and validation of cluster analysis. J. Comput. Appl. Math. 20, 53–65. http://dx.doi.org/10.1016/0377-0427(87)90125-7.

Sayre, R., Dangermond, J., Frye, C., Vaughan, R., Aniello, P., Breyer, S., Cribbs, D., Hopkins, D., Nauman, R., Derrenbacher, W., et al., 2014. A new map of global ecological land units—an ecophysiographic stratification approach. Wash. DC: Assoc. Am. Geogr. 46, http://dx.doi.org/10.13140/2.1.2167.8887.

Simensen, T., Halvorsen, R., Erikstad, L., 2018. Methods for landscape characterisation and mapping: A systematic review. Land Use Policy 75, 557–569. http://dx.doi.org/10.1016/j.landusepol.2018.04.022.

Torres, A., Serra, J., Llopis, J., Delcampo, A., 2020. Color preference cool versus warm in nursing homes depends on the expected activity for interior spaces. Front. Archit. Res. 9 (4), 739–750. http://dx.doi.org/10.1016/j.foar.2020.06.002.

Trop, T., 2017. From knowledge to action: Bridging the gaps toward effective incorporation of landscape character assessment approach in land-use planning and management in Israel. Land Use Policy 61, 220–230. http://dx.doi.org/10.1016/j.landusepol.2016.10.052.

Turner, M.G., 2010. Disturbance and landscape dynamics in a changing world. Ecol. 91 (10), 2833–2849. http://dx.doi.org/10.1890/10-0097.1.

Turner, M.G., Gardner, R.H., 2015. Landscape Ecology in Theory and Practice: Pattern and Process. Springer Science Business Media, Inc.

Uzun, O., Dilek, F., Çetinkaya, G., Erduran, F., Açıksöz, S., 2011. National and regional landscape classification and mapping of Turkey: Konya closed basin, Suğla lake and its surrounding area. Int. J. Phys. Sci. 6 (3), 550–565.

Van Eetvelde, V., Antrop, M., 2009. A stepwise multi-scaled landscape typology and characterisation for trans-regional integration, applied on the federal state of Belgium. Landsc. Urban Plan. 91 (3), 160–170. http://dx.doi.org/10.1016/j.landurbplan.2008.12.008.

Wang, N., Xue, J., Peng, J., Biswas, A., He, Y., Shi, Z., 2020. Integrating remote sensing and landscape characteristics to estimate soil salinity using machine learning methods: A case study from Southern Xinjiang, China. Remote. Sens. 12 (24), http://dx.doi.org/10.3390/rs12244118, URL: https://www.mdpi.com/2072-4292/12/24/4118.

Warnock, S., Griffiths, G., 2015. Landscape characterisation: The living landscapes approach in the UK. Landsc. Res. 40 (3), 261–278. http://dx.doi.org/10.1080/01426397.2013.870541.

Wascher, D.M., 2005. European Landscape Character Areas: Typologies, Cartography and Indicators for the Assessment of Sustainable Landscapes. Technical Report, Landscape Europe.

Yang, D., Gao, C., Li, L., Van Eetvelde, V., 2020. Multi-scaled identification of landscape character types and areas in Lushan National Park and its fringes, China. Landsc. Urban Plan. 201, 103844. http://dx.doi.org/10.1016/j.landurbplan.2020.103844.

Zhang, J., Li, S., Li, M., 2010. A comparison of self-organizing feature map clustering with TWINSPAN and fuzzy C-means clustering in the analysis of woodland communities in the Guancen Mts, China. Community Ecol. 11 (1), 120–126. http://dx.doi.org/10.1556/comec.11.2010.1.17.

Zhao, H., Fang, Y., Xu, X., 2024. Quantifying morphology evolutions of urban heat islands and assessing their heat exposure in a metropolis. Sustain. Cities Soc. 102, 105244. http://dx.doi.org/10.1016/j.scs.2024.105244.

Zhao, W., Ma, J., Liu, Q., Song, J., Tysklind, M., Liu, C., Wang, D., Qu, Y., Wu, Y., Wu, F., 2023. Comparison and application of SOFM, fuzzy c-means and k-means clustering algorithms for natural soil environment regionalization in China. Environ. Res. 216, 114519. http://dx.doi.org/10.1016/j.envres.2022.114519.